Anisotropic electron distribution functions and the transition between the Weibel and the whistler instabilities

F. Pegoraro, L. Palodhi, F. Califano

5^{th} INTERNATIONAL CONFERENCE
ON THE FRONTIERS OF PLASMA PHYSICS AND TECHNOLOGY
18-22 April 2011, Singapore.

Dipartimento di Fisica Università di Pisa pegoraro@df.unipi.it

References

This presentation is based on the PhD thesis of **Lopamudra Palodhi** : "Weibel and Whistler Modes in Vlasov Plasma" (Pisa, July 2010) under the supervision of Prof. F. Pegoraro and on the following articles:

L. Palodhi, F.Califano, F.Pegoraro, Plasma Phys. Contr. Fus., **51**, 125006, 2009.

L. Palodhi, F.Califano, F.Pegoraro, Plasma Phys. Contr. Fus., **52**, 095007, 2010.

See also: *Electrons go for a twist, Plasma Phys. Contr. Fus., LabTalk, 2011. http://iopscience.iop.org/0741-3335/labtalk-article/45158?labTalkTab=mostRead*

Introduction

The relaxation of an anisotropic electron distribution function in a plasma generates a range of coherent electric and magnetic fields.

The nonlinear dynamics of multi-particle systems with long-range forces, such as electrons and ions in a plasma or stars in a galaxy, leads to the formation of long-lived, spatially coherent structures. Such structures generally arise under conditions that are far from thermodynamic equilibrium.

How such systems evolve, whether they relax through the onset of collective instabilities and what type of configurations they evolve towards are longstanding problems of basic importance for physics.

Anisotropy of the particle distribution in momentum space is a ubiquitous feature of both space and laboratory plasmas that indicates absence of thermodynamic equilibrium.

In an unmagnetized plasma such an anisotropy can give rise to the Weibel instability[1] which generates a quasistatic magnetic field.

If an ambient magnetic field is present the Weibel instability turns into the whistler instability [2] and circularly polarized whistler waves are generated.

Above a threshold value of the ambient magnetic field the instability is suppressed.

[1] Weibel E., *Phys.. Rev. Lett.*, **2**, 83 (1959).
[2] Gary S. P. *et al.*, *J. Geophys. Res.*, **111**, A11224 (2006).

Numerical codes that integrate the Vlasov-Maxwell system in phase space in Eulerian coordinates show that the process of “relaxation” of the electron distribution function as the Weibel-whistler instability develops is far richer than simple isotropisation.

The electron distribution becomes twisted in momentum space and modulated in physical space due to the combined forces of the instability and ambient fields.

This leads to the excitation of electromagnetic and electrostatic modes at the first few harmonics of the plasma frequency and, for a large ambient magnetic field, to long wavelength, spatial modulations of the magnetic field generated by the whistler instability (whistler “oscillitons”).

Whistler instabilities, bursts of whistler noise and coherent whistler wave packets have been reported in space and in the Earth's environment[3].

Whistler waves propagate along the ambient magnetic field in the frequency range of $\Omega_{ci} < \omega < \Omega_{ce}$, with Ω_{ci} - Ω_{ce} the electron - proton cyclotron frequencies.
A sufficiently large temperature anisotropy in a magnetized plasma is the most commonly observed mechanism for the generation of whistler waves, but additional mechanisms, such as trapped particle loss cone distributions, can also generate these modes.

Magnetic field generation in a plasma is one of the most important problems for both laboratory and astrophysical plasmas. Several mechanisms of magnetic field generation have been analysed that are effective in different plasma regimes.

In collisionless regimes the Weibel instability can efficiently generate magnetic fields in plasmas with an anisotropic electron temperature distribution.

[3] Contel Le O. *et al., Ann. Geophys.*, **27**, 2259 (2009), Dubinin E. M. *et al., Ann. Geophys.*, **25**, 303 (2007).

The similar filamentation instability (or beam-Weibel instability) occurs when counter streaming beams play the role of the anisotropy and has been widely studied in the literature.
The filamentation instability has been proposed as a mechanism to magnetize the early universe, to provide strong magnetic fields for the afterglow emission of gamma-ray bursts and supernovae explosions[4], and to explain the heating processes in the pulsar winds[5]. The filamentation instability has been also investigated in order to explain the generation of quasistatic magnetic fields in the interaction of ultrashort and ultraintense laser pulses with an underdense plasma[6].

[4] Medevedev M. V. *et al.*, 2006 *Astrophys. J.* **642** L1, Medevedev M. V., Loeb A 1999 *Astrophys. J.* **526** 697, Medevedev M. V. 2007 *Astrophys. and Space Science* **307** 245.

[5] Arons J. 2008 *AIPC* **983** 200.

[6] Askar'yan G.A., *et al.*, 1994 *JETP Letters*, **60**, 240, Askar'yan G.A., *et al.*, 1995 *Comm. Plasma Phys.. Contr. Fus.*, **17**, 35, Califano F., *et al.*, 2001 *Phys.. Rev. Lett.*, **86**, 5293.

Califano F. *et al.*, 1997 *Phys.. Rev. E* **56** 963, Califano F. *et al.*, 2002 *Phys.. Plasmas* **9** 451,
Califano F. *et al.*, 1998 *Phys.. Rev. E* **57** 7048
Davidson R. C. *et al.*, 1972 *Phys. Plasmas* **15** 317
Rowlands G. 2007 *NJP* **9** 247
Dieckmann M. E. *et al.*, 2008 arXiv:0810.5267
Honda M. *et al.*, 2000 Plasma Phys.. Contr. Fusion **50** 025002
Sakai J. I.*et al.*, 2004 *Phys.. Lett. A* **330** 384
Murakami M., Lidsky L. M. 1970 *Phys.. Rev. Lett.* **24** 7
Bret A. *et al.*, 2007 *Phys.. Plasmas* **14** 032103
Stockem A. *et al.*, 2008 *Plasma Phys.. Control Fusion* **50** 025002
Lee, K. F. 1969 *Phys.. Rev.* **181** 447
....

Linear theory

Weibel instability $B_0 = 0$

$|\omega| \gg k_{||} v_{the||}, \quad v_{the\perp} \gg v_{the||}, \quad \gamma \sim [k v_{the\perp}/(1 + k^2 d_e^2)], \quad \omega_r = 0$

more generally in the presence of a weak ambient magnetic field
$\omega_r \leq \gamma, \quad (v_{the,\perp}/c)^2 > (\omega_{ce}/\omega_{pe})^2.$

whistler instability $B_0 \neq 0, \quad (\omega_{ce}/\omega_{pe})^2 > (v_{the,\perp}/c)^2$

$v_{the\perp} \gg v_{the||}, \;\; \omega \gg (k_{||} v_{the||}), \;\; A \equiv (v_{the,\perp}/v_{the,||})^2 - 1$

$\omega_r = \omega_{ce}(kc/\omega_{pe})^2[1 + A(\omega_{pe}/\omega_{ce})^2(v_{the||}/c)^2]$ (parallel propagation, $kd_e \ll 1$),
$\gamma \sim [(k v_{the\perp})^2 - (\omega_{ce}\omega_{pe})^2/2]^{1/2}$
(the threshold condition can be rewritten in terms of the plasma β).

Nonlinear development and numerical results

At low ambient magnetic field, the nonlinear development of the whistler instability is similar to that of the Weibel instability, since the perturbed magnetic fluctuations are much larger than the ambient magnetic field.
However, when the ambient magnetic field is sufficiently strong, the long term nonlinear behaviour of the instability changes drastically.

In both limits the isotropisation of the electron distribution function due to the onset of the instabilities is accompanied by the development of high frequency (Langmuir wave) electron density modulations.

These density modulations are forced by the spatial modulation of the magnetic energy density at wave numbers roughly two times the wave numbers of the most unstable Fourier components of the primary instabilities.

These density modulations become weaker as the ambient magnetic field is increased.

A purely kinetic effect is also present in the small B_0 limit where the development of the Weibel instability leads to strong deformations of the electron distribution function in phase space.

These deformations arise from the differential rotation in velocity space of the electrons around the magnetic field produced by the Weibel instability and generate short wavelength Langmuir modes that form highly localized electrostatic structures corresponding to jumps of the electrostatic potential.

These kinetic effects become weaker and eventually disappear as the ambient magnetic field is increased.

In the case of the whistler instability, low-frequency density modulations involving the proton dynamics occur and generate soliton type structures known as whistler oscillitons.

Oscillitons are coherent nonlinear structures that occur in dispersive media for which the curves of the phase and group velocities cross for a finite value of the oscillation wavenumber k.

Whistler oscillitons are of special importance as they have been invoked in order to describe coherent wave emission in the whistler frequency range observed in the Earth's plasma environment[7].

[7] Sauer K. *et al.*, 2002 Wave emission by whistler oscillitons: Application to "coherent lion roars", *Geophys. Res. Lett.* **29** 2226.

Sydora R. D. *et al.*, 2007 Coherent whistler waves and oscilliton formation: Kinetic simulations, *Geophys. Res. Lett* **34** L22105.

Normalizations and simulation data

In the numerical solutions all parameters are normalized.
We use the plasma frequency ω_{pe} and the velocity of light c as characteristic frequency and velocity.
The electron skin depth $d_e \equiv c/\omega_{pe}$ is the characteristic length scale.
The electric and magnetic field are normalized to $E = B = m_e c\, \omega_{pe}/e$.
The electron temperature is normalized to $m_e c^2$.

The number of grid points in coordinate space is $N_x = 1024$ and the length of the system is $L_x = 10\pi$ in units of the electron skin depth d_e.
The total number of grid points in velocity space is $N_{vx} = 101, \;\; N_{vy} = N_{vz} = 71$.
The system is evolved up to the time $t = 1200\, \omega_{pe}^{-1}$ with a time step $10^{-3} < dt < 10^{-2}$.
The total number of perturbed modes at $t = 0$ is $N = 220$.
The spatial grid spacing is $dx = 0.03$.

Numerical modelling I

- Vlasov-Maxwell code, uses
  - Time splitting scheme
  - Van Leer interpolation method

Time splitting scheme(TSS)

Initial Vlasov equation is splitted into two partial derivative equations, one in (x, t) and the other in (v, t).
The free streaming term :

$$\frac{\partial f}{\partial t} + \vec{v}.\frac{\partial f}{\partial \vec{x}} \quad = 0 \tag{5}$$

and the acceleration term:

$$\frac{\partial f}{\partial t} - \frac{e}{m} \;\; \vec{E} + \vec{v} \times \vec{B} \;\; .\frac{\partial f}{\partial \vec{v}} = 0 \tag{6}$$

Weibel instability

- 1D-2V configuration.
-

$$\frac{\partial B_z}{\partial t} = -\frac{\partial E_y}{\partial x}$$
$$-\frac{\partial B_z}{\partial x} = \frac{\partial E_y}{\partial t} + J_y$$
$$\frac{\partial^2 \phi}{\partial x^2} = -\rho,$$

simulation parameters
- $T_y/T_x = 12$
- $v_{th_{\parallel e}} = 0.02$
- $a_{in} = 10^{-3}$ to 10^{-5}
- $10^{-6} \le \epsilon \le 10^{-4}$
- $\lambda_D = 0.02\, d_e$
- $L_x = 6\pi d_e$
- $B_0 = 0$

-

$$f_e(x, v_x, v_y, t=0) = f_M(v_x, v_y)[1 + \epsilon \sum_{n=1}^{N} \cos(k_n x + \phi_n))]$$

-

$$f_M(v_x, v_y) = \frac{n}{\pi\sqrt{T_x T_y}} exp\Big(-\frac{v_x^2}{T_x} - \frac{v_y^2}{T_y}\Big)$$

-

$$B_z = \sum_{n=1}^{N} a_{in}\ [\cos(k_n x + \psi_n)]$$

Whistler instability

- 1D-3V
- $B_0 \neq 0$
- $$\frac{\partial}{\partial t}(E_y \pm B_z) \pm \frac{\partial}{\partial x}(E_y \pm B_z) = \mp j_y$$
$$\frac{\partial}{\partial t}(E_z \pm B_y) \mp \frac{\partial}{\partial x}(E_z \pm B_y) = \mp j_z$$
$$\frac{\partial^2 \phi}{\partial^2 x} = -\rho$$

simulation parameters

- $T_y/T_x = 12$
- $v_{th_{\parallel e}} = 0.02$
- $a_{in} = b_{in} \sim 10^{-4}$
- $10^{-6} \leq \epsilon \leq 10^{-4}$
- $\lambda_D = 0.03\, d_e$
- $L_x = 10\pi d_e$
- $B_0 = 0.02, 0.1, 0.5$
- $\beta_{\parallel e} = 1,4 \times 10^{-2}, 1.6 \times 10^{-3}$

- $$f_e(x, v_x, v_y, v_z, t=0) = f_M(v_x, v_y, v_z)[1+\epsilon \sum_{n=1}^{N} \cos(k_n x + \phi_n))]; \qquad k_n = 2\pi n/L_x$$
- $$f_M(v_x, v_y, v_z) = \frac{n}{(\pi)^{3/2}\sqrt{T_x T_y T_z}} exp\Big(-\frac{v_x^2}{T_x} - \frac{v_y^2}{T_y} - \frac{v_z^2}{T_z}\Big)$$
- $$B_y = \sum_{n=1}^{N} a_{in}\,[\cos(k_n x + \psi_n)], \qquad B_z = \sum_{n=1}^{N} b_{in}\,[\cos(k_n x + \Upsilon_n)]$$

Weibel mode

$B_{z,k}$ - perturbed magnetic field, $E_{x,k}$ - electrostatic field , $E_{y,k}$ - induced electric field

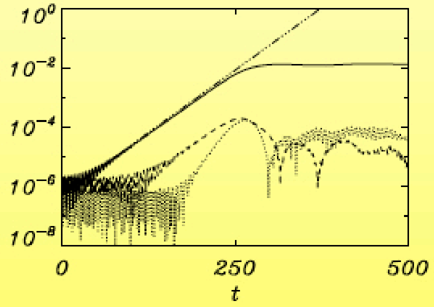

growth of the fields in an unmagnetized plasma

- magnetic field, $k_{max} = 1$, $\gamma_{max} \sim 0.04$
- electrostatic field - coupling between Weibel instability and Langmuir modes, $k_{max} = 2.3$ at $2\gamma_{max}^{Weibel}$

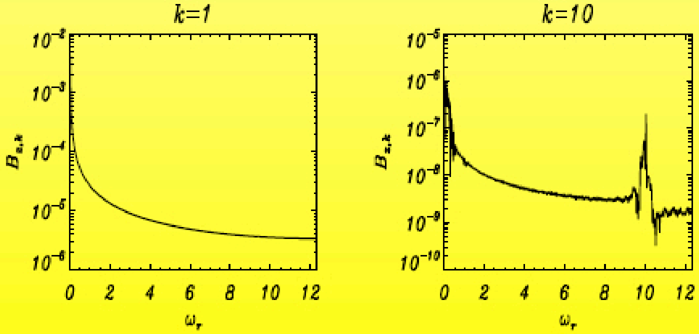

low k - propagation without any oscillations, $\omega_r = 0$
high k - electromagnetic wave, $\omega_r \sim k$

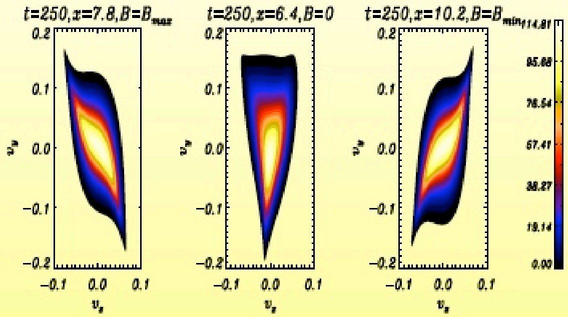

Linear regime:

- ⋆ Differential rotation, $|B_z|$ is maximum
- ⋆ Y-shaped deformation when $B_z = 0$ which means E_y is maximum
- ⋆ Rotation of distribution function depends on the sign of $B_z(B_{max}, B_{min})$
- ⋆ Y-shaped deformation depends on the sign of E_y .

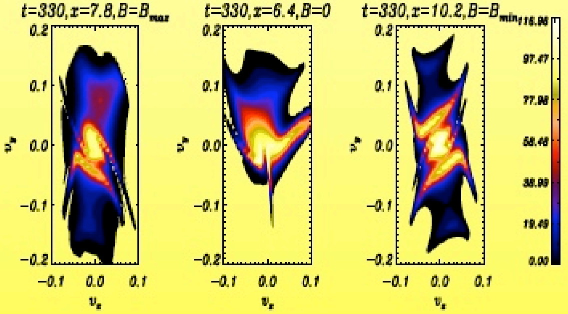

Nonlinear phase:

- ⋆ Winding of the distribution function is tighter
- ⋆ Y-shaped deformation more marked
- ⋆ Ultimately leading to "multi-armed" structures

combined effects of magnetic and induced field !!
electron orbit is deflected when B_z is maximum or E_y vanishes, and E_y accelerates or decelerates the electrons

VISUALIZATION ??

computed set of particle orbits - direct integration of the particle equation of motion in the elctromagnetic fields obtained from the Vlasov integration significance of "multi-armed structures" in the nonlinear phase

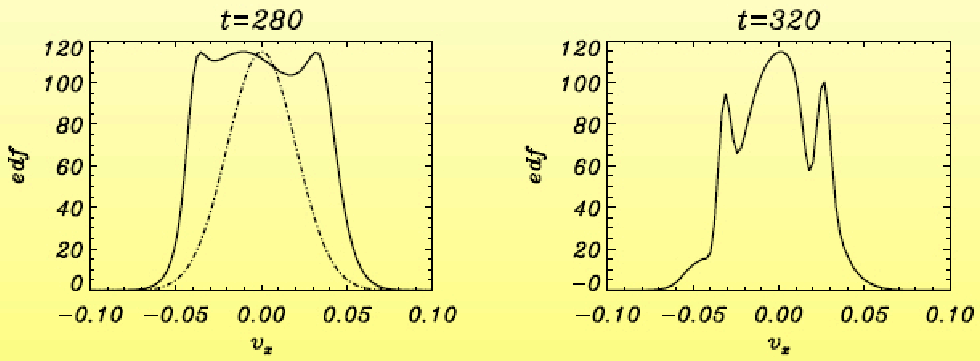

distribution function develops steep positive slopes for velocities of the order of the thermal velocity along x.

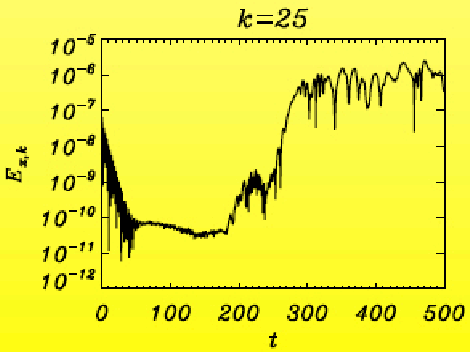

- ⋆ slopes become steeper as distribution function becomes twisted.
- ⋆ $v_{ph} = 0.04$, $\omega_r = 1$, $k = 25$
- ⋆ excitation of Langmuir waves with smaller phase velocities
- ⋆ damping in the initial phase.
- ⋆ non monotonic feature of the EDF makes the mode grow, $\gamma = 0.15$
- ⋆ rate of growth is much larger than the low k Langmuir modes.
- ⋆ leads to highly structured electron density modulations

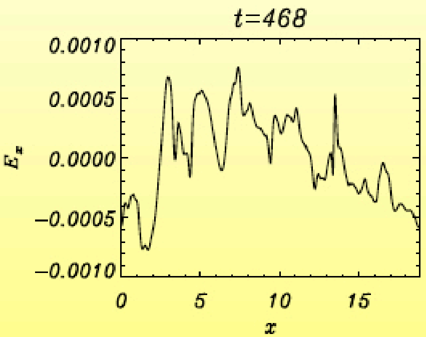

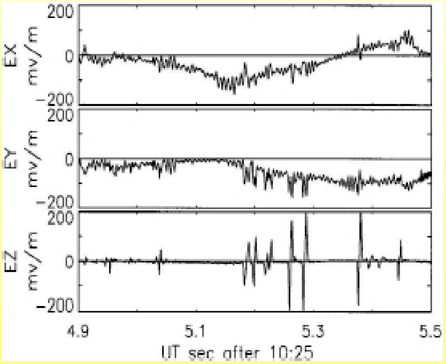

electric field measurements in the auroral acceleration region by Polar Satellite as observed on 10 July 1996.

F. S. Mozer et. al. *Phys. Rev. Lett.*, **79**, 1997

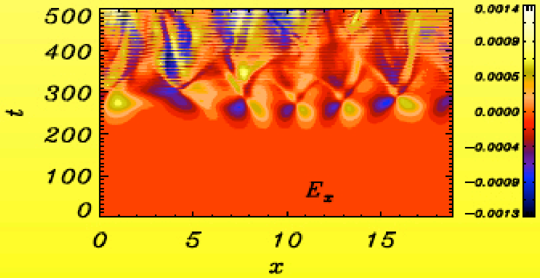

⋆ several narrow spikes, prominant at $x \sim 13.6$.
⋆ correspond to "multi layer" electrostatic structures
⋆ generally accompanied by potential drop.
⋆linear phase: $t = 250$, large sclae structures.
⋆ nonlinear phase: sowly propagating small scale structures on the Debye length scale.
⋆ interact with each other leading to the coalescence.
⋆ at lower temperature anisotropy $T_{\perp e}/T_{\|e} = 4$ structure formation not observed.

Transition from low to high magnetic field

Weibel like mode possibility(Non-resonant)

$$\omega_r \leq \gamma\,, \qquad (v_{th_{\perp e}}/c)^2 > (\omega_{ce}/\omega_{pe})^2$$

Analytical invsetigations:
Lazar et al. *Phys. of Plasmas*, **16**, 2009

Resonant whistler modes

$$\omega_{ce} > \omega_{pe}\sqrt{(A+1)}v_{th_{\parallel e}}/c$$

Linear phase of the simulation - physical quantities

Instability	B_o	ω_{pe}/ω_{ce}	k_{max}	γ_{max}^{Ana}	γ_{max}^{Num}	$\hat{B}_z$	$\beta_{\parallel e}$	$\beta_{\perp e}$	ω_r^{Ana}
Weibel	0.0	-	1.0	0.034	0.037	-	-	-	0
Whistler	0.02	50	1.2	0.037	0.038	2.25	1	11.75	0.02
	0.10	10	1.2	0.031	0.035	0.56	0.04	0.50	0.08
	0.50	2	2.0	0.025	0.020	0.06	0.0016	0.02	0.47

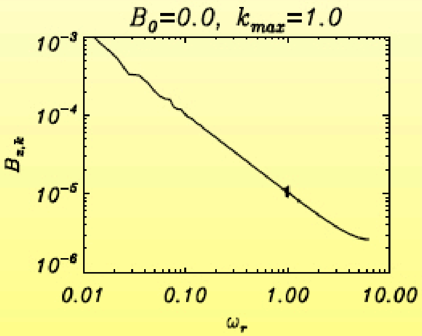

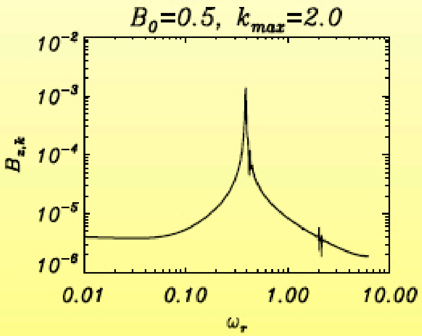

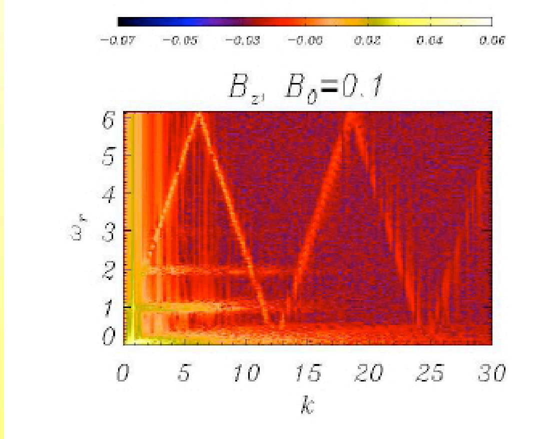

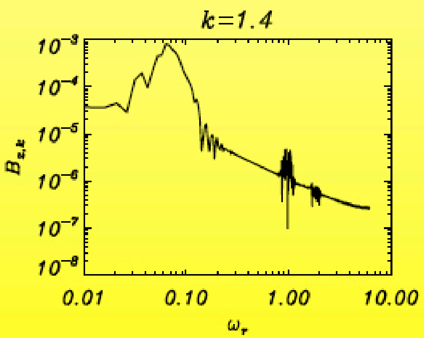

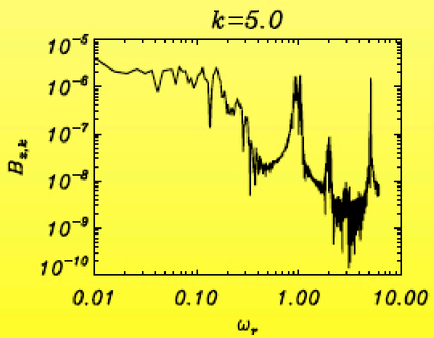

$\mathrm{B}_0 = 0.1$

⋆ whistler frequency at $\omega_r = 0.45$ for $B_0 = 0.5$ and $\omega_r = 0$ when $B_0 = 0$.
⋆ whistler modes become stronger with increasing magnetic field
⋆ presence of waves at ω_{pe} in both low and high magnetic field cases.
⋆ $\omega_r = 0.07$ for $B_0 = 0.1$, wave at $2\omega_{pe}$
⋆ at high k electromagnetic wave is also present $\omega_r \sim k$
⋆ amplitude of $2\omega_{pe} < \omega_r$
⋆ electromagnetic waves is the strongest.

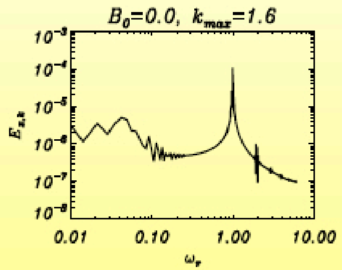

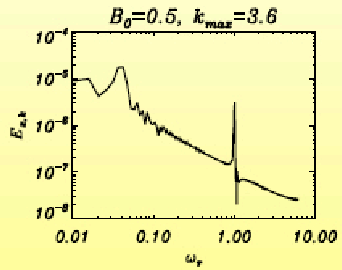

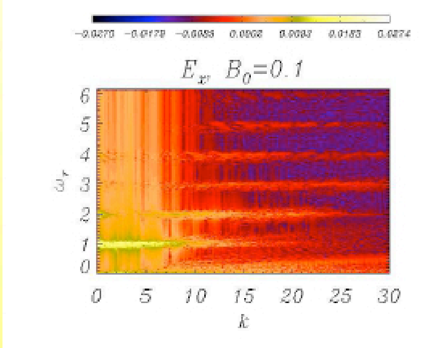

peak at very low frequency - interesting !!

⋆ waves at plasma frequency
⋆ waves present at multiple harmonics upto $6\omega_{pe}$
⋆ with increasing harmonic number relative intensity decreases.

⋆ interestingly, for $B_0 = 0.5$ such higher harmonics are not observed.
⋆ also true for magnetic field
⋆ solar wind, $\omega_{ce}/\omega_{pe} \sim 10^{-2}$, i.e., $B_0 = 0.02, 0.1$ situation for emission.

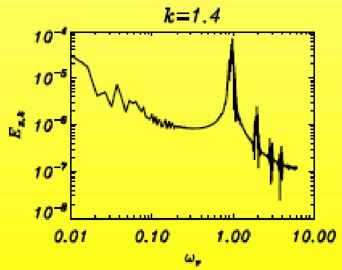

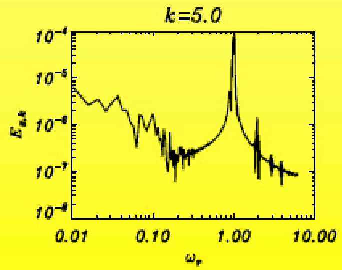

$\mathbf{B_0 = 0.1}$

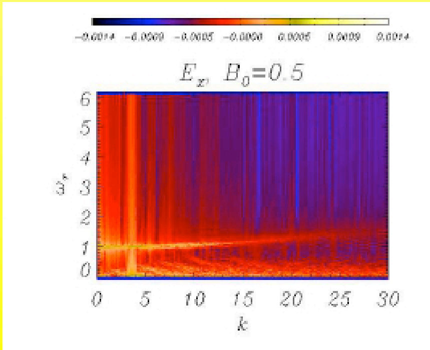

Electrostatic structures and distribution function

Higher wavenumbers:

1. Electrostatic structures formed at modes k larger than those of whistler modes
   1.1 $B_0 = 0$, $v_r = 0.05$, Excitation of Langmuir waves with wave mode $k \sim \omega_r / v_r \sim 20$
   1.2 $B_0 = 0.1$, $k \sim 10$.
2. Deformation of the distribution function due to the differential rotation of the magnetic field generated in the $y - z$ plane.
3. Deformation becomes weaker as ambient magnetic field increases.
4. Electrostatic structures formed at lower magnetic fields
   4.1 Amplitude of 1D-3V structures are less than 1D-2V.
   4.2 Initially randomly oriented perturbed magnetic field becomes organized in $y - z$ plane.

- Smaller wavenumbers - Interplay between perturbed magnetic field amplitude and of the electron and proton densities.
  - Long wavelength modulations of the electrostatic structures and the electron and proton densities at half the wavelength of the magnetic field.
  - The wavelength of the modulations of both the magnetic field and of the proton and electron densities decreases with increasing magnetic field.
  - The electrostatic and density modulation wavelength equal to half the wavelength of the most unstable Fourier component of the perturbed magnetic field.

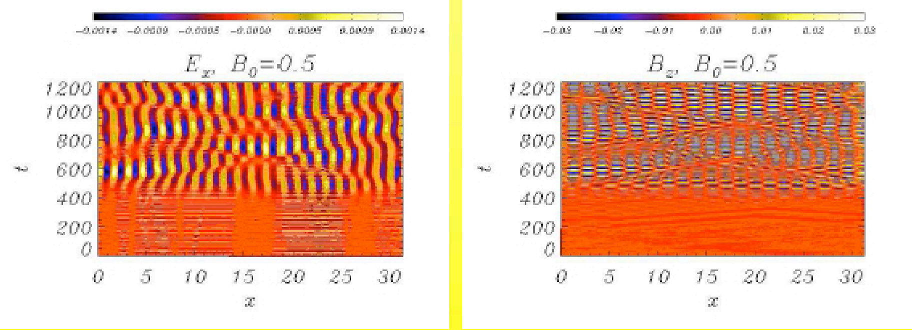

forward and backward propagating waves

dominant whistler waves are modulated by the low frequency perturbations observed in the electrostatic field

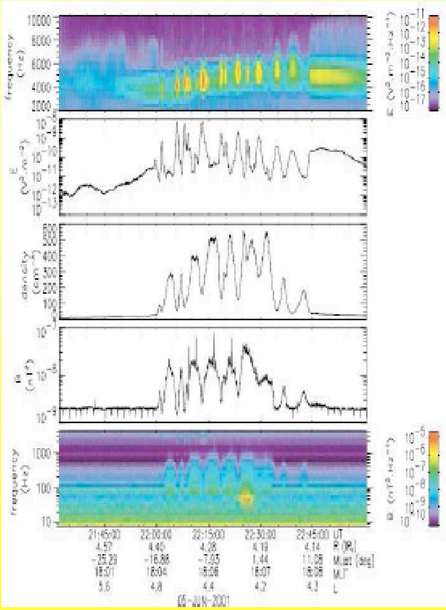

WHISPER C3 on June 5, 2001
from 21:32 UT to 23:15 UT
O. Moullard et. al. *Phys. Rev. Lett.*, **29**, 2002

- two kind of modulations in magnetic field
- long wavelength - $L \sim 17$, $T \sim 200$, $v_{ph} \sim 0.08$.
- short wavelength - $L \sim 2$, $T \sim 7$, $v_{ph} \sim 0.28$.
- long wavelength phase velocity falls in the range of whistler phase velocity
- also comparable with some of the phase velocities obtained from short wavelength($0.005 \leq v_{ph} \leq 0.01$) and long wavelength($0.075 \leq v_{ph} \leq 0.13$) electrostatic modulations.
- phase velocity range $0.08 \leq v_{ph} \leq 0.01$ obtained from low frequency peak $0.03 \leq \omega_r \leq 0.04$ in electrostatic frequency spectrum at $k_{max} = 3.6$ covers large part of whistler phase velocity range.
- ponderomotive force due to the interaction of the whistler packets and low density perturbations.

theory !! nonlinear coupling of opposite travelling waves produces low frequency ponderomotive force with $\omega = \omega_1 - \omega_2$ and $k = k_1 - k_2$.
L. Stenflo et. al. *J. Geophys, Res.*, **91**, 1986

Nonlinear structure formation: wave packets

- wave packets are generated by the oscillitons.
- oscillitons: oscillations within solitons.
- in the whistler range are called whistler oscillitons.
- arise from the momentum exchange between protons and electrons.
- electron and proton cavities are formed.
- existence of a 'resonant point' where group velocity and phase velocity coincides.
- modifies the frequency range of the whistlers - shift of the broad magnetic spectrum to lower k vlaues.

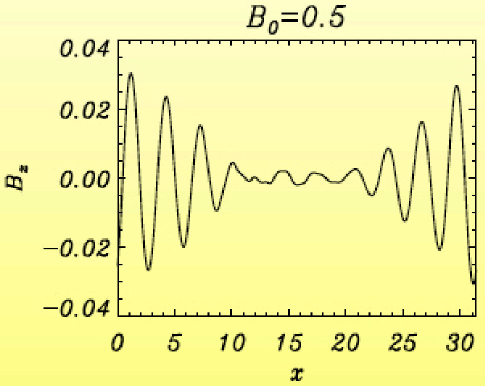

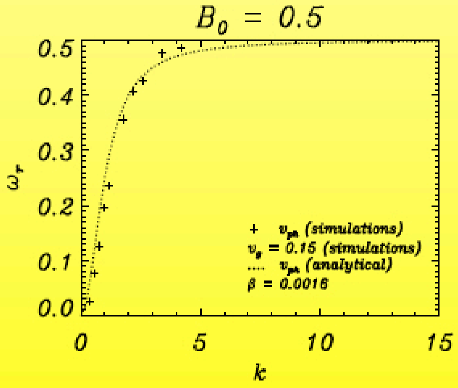

CLUSTER observations are available from Earth's plasma environment
O. Moullard et. al. *Phys. Rev. Lett.*, **29**, 2002

Conclusions

Pressure anisotropy provides the free energy source for the development of the Weibel instability and the generation of a quasi-static magnetic field in an unmagnetized plasma.

This instability causes a violent deformation of the electron distribution function in phase space leading to the generation of short wavelength Langmuir modes. This mechanism coexists with the ‘fluid-like’ generation of longer wavelength Langmuir modes due to the nonlinear modulation of the electron density.

This mechanism corresponds to a non-local energy transport between modes in wave-number space. Eventually these short wavelength Langmuir modes lead to the formation of highly localized electrostatic structures. These structures correspond to potential jumps and are of interest for space observations.

As we move towards higher ambient magnetic fields, ω_r becomes comparable to the maximum growth rate of the instability. At very high ambient magnetic field ($B_0 = 0.5$, being the value of the electron cyclotron frequency normalized to the Langmuir frequency) the mode becomes resonant with ω_r much larger than the growth rate (whistler instability).

The development of these instabilities is accompanied by the generation of electrostatic and electromagnetic waves at the harmonics of the plasma frequency (up to the fifth harmonic in the case of the electrostatic spectrum). These secondary phenomena tend to be suppressed as the ambient magnetic field becomes larger.

In contrast, at large ambient magnetic field we find a low-frequency long wavelength modulation of the whistler wave spectrum that we interpret in terms of the self-consistent interaction between the perturbed magnetic field and the low frequency electron and proton density modulations (whistler oscillitons)